Trends in Parasitology

CellPress OPEN ACCESS

Opinion

Extraordinary parasite multiplication rates in human malaria infections

Megan A. Greischar [1,*] and Lauren M. Childs [2]

For pathogenic organisms, faster rates of multiplication promote transmission success, the potential to harm hosts, and the evolution of drug resistance. Parasite multiplication rates (PMRs) are often quantified in malaria infections, given the relative ease of sampling. Using modern and historical human infection data, we show that established methods return extraordinarily – and implausibly – large PMRs. We illustrate how inflated PMRs arise from two facets of malaria biology that are far from unique: (i) some developmental ages are easier to sample than others; (ii) the distribution of developmental ages changes over the course of infection. The difficulty of accurately quantifying PMRs demonstrates a need for robust methods and a subsequent re-evaluation of what is known even in the well-studied system of malaria.

Highlights

Theory assumes that multiplication rates of pathogenic organisms have substantial influence on disease severity and spread.

Malaria infections represent one of the most straightforward systems in which to measure parasite multiplication rates (PMRs), but PMRs have proven difficult to link to health outcomes.

Applied to human infection data, standard methods for estimating PMRs yield extraordinarily large values, far exceeding the maximum expansion rate (i.e., burst size) established *in vitro*.

Spurious multiplication rates appear when some ages of parasites are more difficult to sample and when the age distribution of the parasite population changes through time, problems that are likely common among pathogenic organisms.

Small changes in age distributions can lead to estimates of extraordinarily high multiplication rates that may explain why PMRs often fail to predict disease severity.

How and why multiplication rates are calculated

The rate at which pathogenic organisms multiply determines their capacity to harm their hosts [1,2] and to evolve traits of concern like drug resistance [3]. Accordingly, substantial effort has gone into characterizing multiplication rates in pathogenic organisms that impose major health burdens, such as malaria parasites (e.g., [4–17]). Despite considerable effort and the comparative ease of sampling blood-borne parasites, it has proven difficult to link faster multiplication rates with disease severity in human malaria infections (reviewed in [18]). The lack of a consistent pattern suggests either a gap in understanding – where faster multiplication does not result in greater pathology due to as yet unidentified reasons – or methodological challenges that prevent accurate estimation of PMRs. The challenge of linking multiplication rates to infection outcomes will only be magnified in pathogenic organisms that are harder to sample.

Multiplication rates are the fold change in numbers over a generation, or for pathogenic organisms, a replicative cycle. Malaria parasites take time, typically a multiple of 24 h that depends on the malaria species [19], to develop and replicate within red blood cells (RBCs) before bursting out of **infected RBCs** (**iRBCs**) (see Glossary) to invade new RBCs and continue the replicative cycle. The **PMR** represents the fold change of the iRBC population over each replicative cycle. For the human malaria parasite *Plasmodium falciparum*, PMR indicates the fold change over 2-day intervals (e.g., [4]), typically estimated either directly from observed iRBC counts (PMR_{obs}) or via log-linear regression (PMR_{reg}), illustrated in Figure 1A,B. Observed PMRs (PMR_{obs} in Equation 1 in Figure 1B) are calculated by taking the observed iRBC count 2 days in the future divided by the present iRBC count. PMRs via linear regression (PMR_{reg} in Equation 2 in Figure 1B) are obtained by linear regression for each patient of $\log_{10}$ iRBC count as a function of day, where m is the determined intercept and b is the slope [5,18]. PMR_{obs} can be estimated whenever the iRBC counts are available from the relevant times (t, $t + 2$) and can change over time to reflect changes in population growth rates over the course of infection. In contrast, PMR_{reg} is only appropriate when iRBC abundance is growing in a log-linear fashion and returns a single, constant population growth rate.

[1]Department of Ecology & Evolutionary Biology, Cornell University, Ithaca, NY, USA
[2]Department of Mathematics, Virginia Tech, Blacksburg, VA, USA

*Correspondence:
megan.greischar@cornell.edu
(M.A. Greischar).

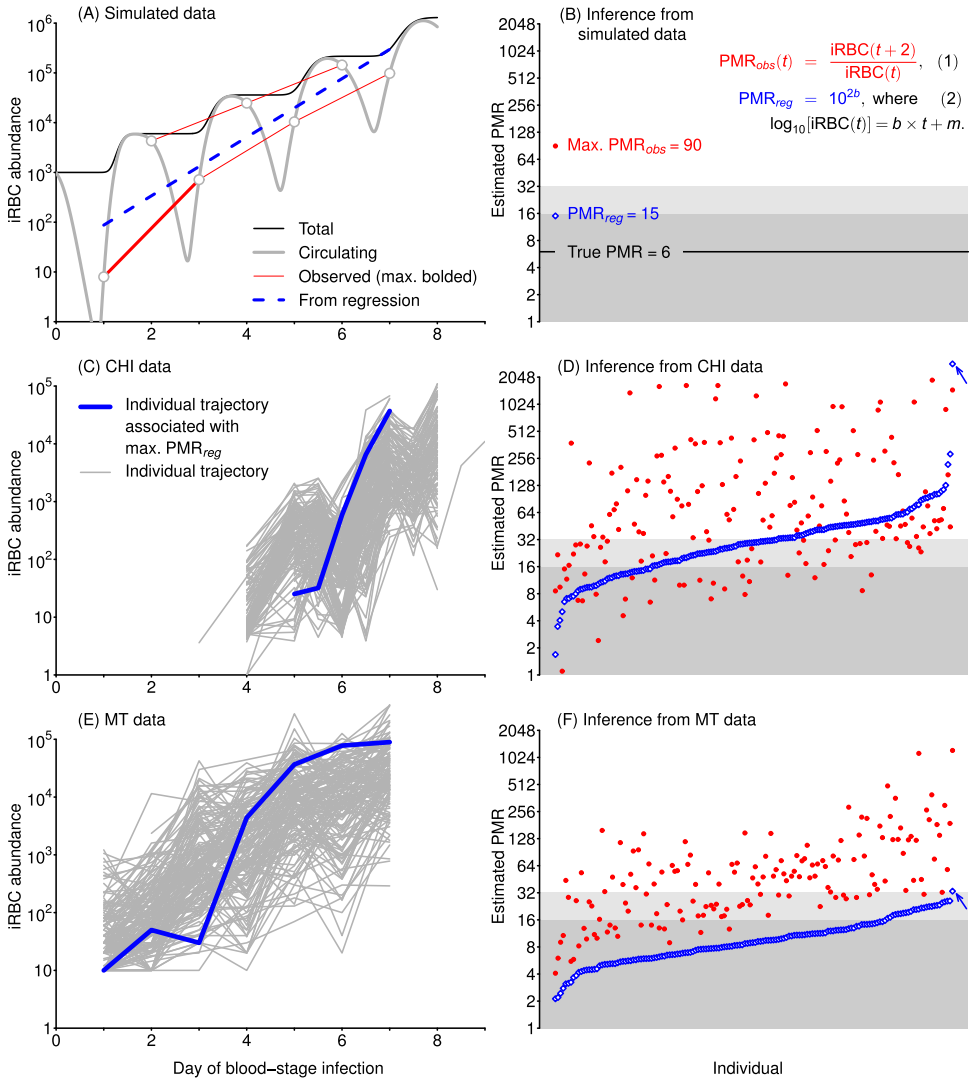

Trends in Parasitology

Figure 1. Methods for estimating parasite multiplication rate (PMR) rely on counts of circulating infected red blood cells (iRBCs), often yielding extraordinary PMRs. (A) Circulating iRBCs (unbroken gray line) represent more or less of the total iRBC population (unbroken thin black line) depending on the timing of sampling (open gray circles). Simulated data assume initial synchrony with a parasite age range spanning 9 h (i.e., 99% of the first wave of bursting occurs over 9 h) and an initial median parasite age of 16 h. PMRs estimated from observed iRBC abundance using Equation 1 are indicated with unbroken red lines (PMR_{obs}, maximum bolded), and PMR from regression using Equation 2 with a broken blue line (PMR_{reg}). (B) Both PMR_{obs} (closed red circles) and PMR_{reg} (open blue diamonds) greatly exceed the true PMR of 6. Individual patient time series used to infer PMRs are shown in gray at left for controlled human infection (CHI) trials (C) and the malariatherapy (MT) data set (E), with the trajectory corresponding to the maximum PMR_{reg} bolded in blue. The corresponding inferred PMRs are shown at right on a logarithmic scale (D and F, respectively). Dark gray rectangles highlight PMRs below 16, a plausible median burst size based on *in vitro* assays [6]. Light gray rectangles indicate values that fall above 16 but below the maximum of 32 [24]. Individual patients are ordered on the horizontal axis by increasing PMR_{reg} with a blue arrow to indicate the maximum PMR_{reg}. Only infections for which both PMR_{obs} and PMR_{reg} could be calculated are shown. See Box S1 in the supplemental information online for code and data used to generate this figure.

While PMRs are conceptually simple to calculate, they rely on repeated, accurate estimates of iRBC abundance within a host. Sequestered iRBCs (Box 1) do not circulate in the blood such that the observed iRBC count represents some fraction of the underlying total iRBC abundance

Glossary

Burst size: the average number of daughter parasites released when an iRBC bursts at the end of intraerythrocytic development. The burst size represents an upper limit on PMRs since not every daughter parasite will necessarily infect another RBC.

Infected RBC (iRBC): a red blood cell (RBC) that has been invaded by one or more parasites. Younger iRBCs tend to circulate while mature iRBCs may sequester where they are difficult to sample.

Intraerythrocytic development: the process of maturation and multiplication by malaria parasites within RBCs. This period of development represents the time from invasion of RBCs to bursting. For *P. falciparum*, the intraerythrocytic development period lasts 48 h.

Parasite multiplication rate (PMR): the fold change in iRBC abundance from one cycle of intraerythrocytic development to the next.

Sequestration: the attachment of iRBCs to capillary walls in the microvasculature as parasite development progresses within them. Sequestered iRBCs are difficult to sample, while circulating iRBCs – those whose parasites are in earlier stages of development – can be readily sampled from the blood.

Synchrony: when the population of parasites within the iRBCs of a host develop in unison, causing discrete waves of RBC bursting and invasion.

Box 1. The problem of sequestration

For many malaria species, including *P. falciparum*, iRBCs become harder to sample later in intraerythrocytic development. Parasites at later developmental ages – approximately 18 h post-invasion of RBCs onwards [28] – sequester (reviewed in [18]), that is, adhere to the microvasculature to avoid clearance by the spleen [4,56]. Depending on the timing of sampling with respect to the schedule of intraerythrocytic development, sequestration means that blood samples may be more or less representative of the total iRBC population. The fraction of the total iRBC population sampled will show the greatest variation through time when intraerythrocytic development is synchronized (Figure I).

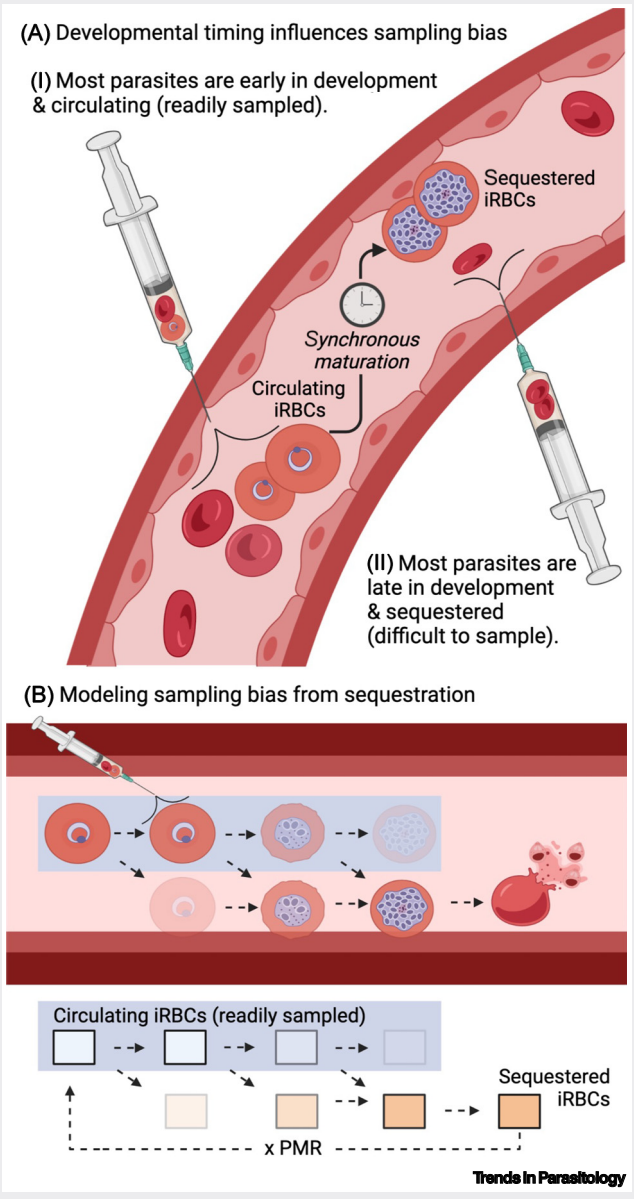

Figure I. Sequestration can bias counts of infected red blood cells (iRBCs). (A) At sampling time I, the parasites within iRBCs are early in intraerythrocytic development, so that the iRBCs circulate freely where they can be readily sampled from a blood draw. Sampling time II follows synchronous maturation of the population of iRBCs within the host, so that most parasites are in later stages of development and iRBCs adhere to blood vessel walls where they cannot be readily sampled (i.e., cannot be taken up when a person is phlebotomized). (B) In the model used here [27] to illustrate how sequestration alters observable infection dynamics, intraerythrocytic development is assumed to occur in parallel over a series of circulating and sequestered iRBC compartments. Circulating developmental phases are shown on a blue background and represent the iRBCs that can be sampled. Greater transparency in iRBCs and corresponding boxes indicates a lower likelihood of iRBCs present (e.g., iRBCs are unlikely to sequester early or circulate late in development). The model allows for gradual and incomplete sequestration but – when parameterized for *Plasmodium falciparum* (following [28]) – implies rapid and complete sequestration around 18 h post-RBC invasion. Abbreviation: PMR, parasite multiplication rate. This figure was created using BioRender.

(Figure 1A), and iRBC counts can vary considerably over short time intervals [20]. Reconstructing the underlying abundance is by no means trivial, since it depends on the age distribution of the parasite population residing within iRBCs and that age distribution is impossible to observe

directly, except from autopsy of fatal cases [21]. When parasite development is highly synchronized and iRBCs containing mature parasites sequester, then iRBC counts oscillate with a period roughly equal to the duration of the replicative cycle, for example, 2 days for *P. falciparum* infections [5,22]. Often a sine wave is fit to these periodic oscillations when PMR is estimated through regression, where the amplitude of the sine wave is used as an estimate of **synchrony** [5]. Critically, these oscillating iRBC counts, whether derived from qPCR or microscopy, represent circulating iRBC counts, not those sequestered in the microvasculature. Therefore, PMRs do not reflect the entire population of iRBCs within a host, and current opinion recommends that PMRs be considered along with other metrics – including a modified PMR calculation that relaxes the assumption of a 48 h life cycle and estimates of total parasite biomass – to understand disease severity [18].

Yet all metrics for quantifying PMR rely on circulating iRBC abundance (reviewed in [18]). In particular, calculations of total parasite biomass are recommended (e.g., estimating circulating and sequestered iRBC abundance through parasite-produced proteins like PfHRP2), but also require estimating multiplication rates [23] (reviewed in [18]). The lack of unbiased alternatives suggests an urgent need to discover precisely why and how estimates of multiplication rates fail to reflect dynamics within the host. In many systems, multiplication rates must be inferred from *in vivo* time series data but some human malaria parasites (in particular, *P. falciparum*) can also be grown in artificial culture, where experiments have characterized the number of daughter parasites each iRBC releases, known as the '**burst size**' [6,24]. The burst size represents an upper limit on parasites' capacity for multiplication and serves as an independent check on PMRs inferred from *in vivo* data.

Multiplication rates should – at most – approach the upper limit defined by burst sizes (32 for *P. falciparum*, [24]). Even under ideal conditions, where all daughter parasites emerging from RBCs are successful, the PMR should fall close to the median burst size (on the order of 15–18, depending on the strain, [6]). Nonetheless, anomalously high multiplication rates have been reported, with model-fitted estimates exceeding median [14] and even maximum [17] burst sizes. PMR estimates from individual patient time series can exceed 100 [15]. These rapid multiplication rates can appear more reasonable – exceeding median if not maximal burst sizes – if life cycle length (i.e., the duration of **intraerythrocytic development**) is fitted and allowed to be shorter than 48 h, ranging from 34 to 45 h [14]. However, expansion rates that exceed median burst sizes are still considerable, and recent work highlights unexpected difficulties in accurately estimating the duration of intraerythrocytic development, including bias caused by **sequestration** [25]. The discrepancy between PMRs and burst sizes, along with the uncertainty surrounding the timing of intraerythrocytic development, raises questions about what is known regarding *in vivo* multiplication rates even in the well-studied system of malaria.

Current methods return extraordinary PMRs from human infection data

We illustrate how sequestration impacts estimates of PMRs using a previously developed model for *P. falciparum* infections [26,27]. Briefly, that model assumes that iRBCs progressively transition from circulating to sequestered as parasites develop within iRBCs using an empirically derived functional form based on data from [28] (details of derivation in [27]). We simulate a synchronous start to the infection, so that circulating iRBC counts oscillate with a 48 h period as observed from human infection data (compare Figure 1A with C and E). We mimic *in vivo* data by using only circulating iRBCs to calculate PMR_{obs} and PMR_{reg} (Equations 1 and 2, respectively), finding that existing methods return spuriously large PMRs (Figure 1B). Perplexingly large PMRs – that often vastly exceed median and even maximum reported burst sizes – likewise emerge when these methods are applied to two sets of human infection data (Figure 1C–F):

(i) modern data from controlled human infection (CHI) trials compiled by [14]; (ii) historical data from 1940–1963 when deliberate infection with malaria parasites was an accepted treatment for neurosyphilis, known as malariatherapy (MT, ethics reviewed in [29]).

Examining individual time series reveals apparently explosive rates of parasite multiplication, even after accounting for other issues like detection limits (Box 2). The iRBC trajectories associated with the maximum PMR_{reg} for each data set (bolded blue in Figure 1C,E) both span three orders of magnitude over a 2-day period, corresponding to PMR_{obs} in excess of 1200. Even excluding these extreme examples, many human infections exhibited extraordinary PMRs, meaning values exceeding the maximum observed burst size for *P. falciparum*, approximately 32 parasites per iRBC (Figure 1). These extraordinary PMRs appear whether the data were obtained from modern CHI trials (Figure 1C,D) or historical MT infections (Figure 1E,F), so do not appear to be an artifact of the method used to quantify iRBC abundance (qPCR or microscopy, respectively). qPCR would be expected to yield greater accuracy in PMRs given the lower detection limit [30], but that data set yields consistently higher PMRs than the historical MT data (compare Figure 1D to F). Simulated time series also refute the notion that extraordinary PMRs are the result of sampling error, since we recover erroneously large PMRs without any error in circulating iRBC counts (Figure 1A,B).

Neither can extraordinary values be tied to the method used to estimate PMR, since PMRs can exceed the plausible upper bound whether derived from observed iRBC counts or estimated from linear regression (Figure 1). While PMR values obtained from regression tend to fall into a narrower range than the maximum observed PMR calculated directly from iRBC abundance, it is still entirely possible to obtain extraordinary PMRs from regression, as we found in more than 40% of CHI infections (Figure 1D). We use maximum observed PMRs to provide a single value for comparison with PMRs obtained from regression, focusing on the maximum values from each infection to illustrate the extreme magnitude of the bias in PMR. The MT data consistently exhibit lower PMRs from regression compared with maximum observed PMRs, in contrast to

Box 2. Additional considerations for estimating PMRs

Beyond sequestration, there are other considerations in estimating PMRs. First, circulating iRBC counts can be estimated with different methods – for example, qPCR or microscopy – that entail distinct detection limits. Near the detection threshold, counts become less reliable [57] and may lead to false zeros and spuriously large PMR estimates. Second, PMRs can be estimated across multiple infections simultaneously or separately for individual infections. Estimating PMRs across multiple infections requires assumptions about distributions of key parameters across patients (e.g., [5]) but can compensate for sampling error in circulating iRBC counts. However, if counts across patients are consistently biased – for example, due to sequestration – that bias may only be apparent from estimating PMRs for individual infections. Finally, obtaining PMRs from regression assumes that the parasite population is expanding in a log-linear manner, and some infections violate that assumption, especially when sampled over a longer time period. We describe how to address these issues using the two data sources shown in Figure 1 in main text.

In the CHI data, circulating iRBC abundance was estimated via qPCR during the acute expansion phase of 177 infections, and iRBC counts are reported as the geometric mean of duplicate or triplicate samples using methods designed to account for a detection limit [14]. Infections were terminated with drug treatment at the last time point sampled [14]. Wockner *et al.* [14] estimate PMR_{reg} across all time series simultaneously with a nonlinear mixed effects model. We instead estimate maximum PMR_{obs} and PMR_{reg} for individual infections (see Figure 1C in main text) to explore bias in existing methods.

The MT data encompass acute and chronic phases of infection, with circulating iRBC counts obtained via microscopy. Simpson *et al.* [5] used regression to estimate PMR for the first 7 days of infection, excluding any infections not showing log-linear expansion of iRBC abundance over that period (e.g., because of drug treatment [5]). The MT iRBC counts are not pre-processed to account for the detection limit (10 iRBCs/μl for microscopy, [5]). Treating any iRBC counts below the detection threshold as missing, we re-estimate PMRs from the MT data following [5], except that Simpson *et al.* calculated PMR_{reg} values for all patients simultaneously assuming a log-normal distribution across patients, and we estimate PMRs for each patient individually. Time series of iRBC counts for all included infections are shown in Figure 1E in main text, while excluded infections (i.e., those not conforming to log-linear expansion) are shown in Figure S1 in the supplemental information online.

the CHI data. That pattern is explained by the fact that regressions of the MT data encompassed 7 days' worth of abundance data, compared to 4 days for the CHI data. Though more time points lessen the impact of large oscillations in circulating iRBC counts (e.g., Figure 1A), regressing the MT data can nonetheless return PMR estimates that exceed median and even maximum burst size estimates (Figure 1F).

Larger than expected PMRs are often explained as the outcome of intraerythrocytic development taking less than the expected 48 h (e.g., approximately 37 or 39 h, [14,17], respectively). To put these extraordinary PMRs in context, even if we assume that intraerythrocytic development requires only 24 h, iRBCs would have to maintain maximum burst sizes for two consecutive cycles to change iRBC abundance across three orders of magnitude over 2 days ($32^2 = 1024$). Maintaining median burst sizes over two 24 h cycles would yield a PMR of $16^2 = 256$, but many PMR_{obs} and some PMR_{reg} still exceed that value, sometimes by an order of magnitude. Of course, deviations from expectation are possible in burst sizes and in the duration of intraerythrocytic development, but these deviations would have to be considerable to explain the PMRs we recover from data. In contrast, we can easily recover extraordinary PMRs merely by simulating sequestration (Figure 1A,B), a well-known aspect of *P. falciparum* biology.

PMR estimates depend on the schedule of intraerythrocytic development

Understanding variation in the developmental schedules of malaria parasites remains a very active area of research (reviewed in [31]), so we illustrate bias in PMRs from simulated time series assuming a range of initial median parasite ages and synchrony levels (i.e., the width of the initial distribution of parasite ages, extremes shown in Figure 2A). We can recapitulate the extraordinarily large PMRs estimated from *in vivo* data even though the true PMR is constant at 6, provided the infection is initially synchronous (Figure 2B). While the maximum PMR_{obs} shows greater extremes than PMR_{reg}, both systematically overestimate the multiplication rate in synchronized infections, with the largest errors in PMR estimates when the initial median parasite age is offset from the sampling time by roughly 12 h (Figure 2B). This offset leads to such significant discrepancies because some of the samples occur when most parasites are sequestered, resulting in severe underestimates of total iRBC numbers at certain time points (see Figure 1A for an example time course). In contrast, the estimates for initially asynchronous infections are close to the true values and do not vary depending on the initial median parasite age (Figure 2C).

Even moderate levels of synchrony generate exaggerated PMRs, but estimates are especially poor with higher levels of synchrony (see Figure S2 in the supplemental information online). Importantly, even the more realistic values remain overestimates, and PMR estimates show worrying sensitivity to the initial median parasite age (relative to sampling) whenever infections begin with some level of synchrony. When simulated infections are synchronized, the deviation from the true value increases with the true PMR, and the worst errors again appear when the median parasite age is 12 h initially (true PMR 2–32, Figure S3 in the supplemental information online). Inflated PMRs are likewise a problem when iRBC populations are undergoing a fold-decrease in numbers, such that declining iRBC numbers can appear as up to a fivefold increase (Figure S4 in the supplemental information online). These spuriously large values again pose practical problems since the fold-decrease in iRBC numbers (i.e., the 'parasite reduction ratio') is used to evaluate antimalarial activity of novel therapeutics [32]. Parasite age distributions at the beginning of sampling are typically unknown for *in vivo* infections, due again to the problem of mature stages sequestering, making it impossible to evaluate whether any particular PMR estimate is likely to fall close to, or far from, the true value.

If synchrony is lost over time, maximum observed and regression PMR estimates should revert to more biologically reasonable values (Figure S5A in the supplemental information online). Because

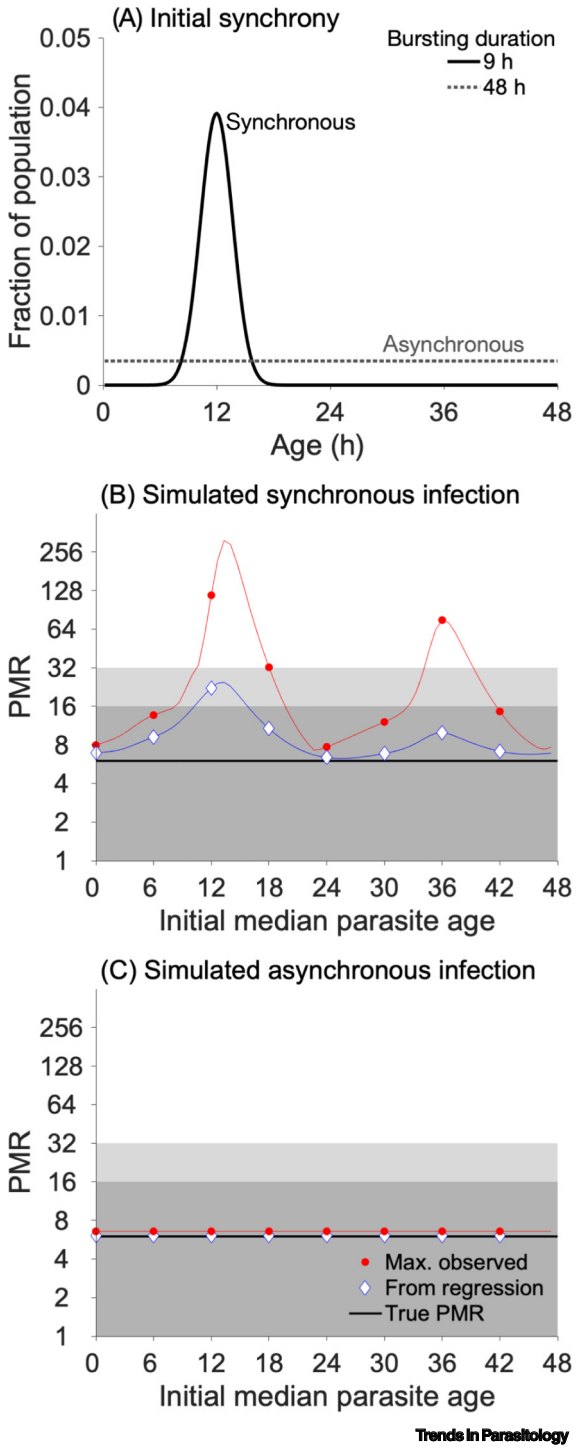

Figure 2. Extraordinary parasite multiplication rates (PMRs) are an artifact of sequestration and changing parasite age structure. (A) PMRs were estimated from simulations with initial synchrony or asynchrony, where synchrony is defined as the hours required for 99% of an infected red blood cell (iRBC) cohort to burst ('bursting duration'). The initial parasite age distribution is assumed to be symmetric beta-distributed with both shape parameters set to the same value, s_p, with larger s_p values indicating more synchronous (i.e., narrower) starting age distributions. The distributions shown as an example assume an initial median parasite age of 12 h post-invasion. (B) PMRs estimated from a simulated synchronous infection regularly exceed the true PMR of 6 (unbroken black line, other colors and symbols as in Figure 1). Deviation from true PMR depends on the median parasite age at the time of sampling (note the logarithmic y-axis scale) but represent overestimates, whether inferred directly (maximum PMR_{obs}) or by regression (PMR_{reg}). (C) PMRs estimated from a simulated asynchronous infection fall very close to the true value. See Box S1 in the supplemental information online for code and data used to generate this figure.

synchrony is decaying, the minimum measurable fraction of iRBC counts will increase with each cycle of intraerythrocytic development (Figure S5B in the supplemental information online), leading to substantial overestimates of the true PMR. PMR estimates should be reasonable once synchrony has decayed into asynchrony and a consistent fraction of the iRBC population is measurable over the course of infection, but that suggests two important quandaries. First, excluding early time points may improve estimates, since extraordinary PMRs are more likely early in infection (max. PMR_{obs}, Figure S6 in the supplemental information online); however, those early dynamics are important for understanding the role of immunity [33], and early time points may represent the entirety of obtainable data from some experiments, such as CHI trials. Second, one solution would seem to be excluding iRBC counts from highly synchronized infections, but synchrony is itself challenging to quantify [31], due in part to sequestration. Even if initially synchronized infections could be identified, it remains unknown how long initially synchronized infections maintain synchrony, and without that information it is impossible to make sensible recommendations about which time points to exclude from analysis. Extraordinary PMRs appear throughout the brief span of time that can be examined in CHI trials and hundreds of days into the MT infections (max. PMR_{obs}, Figure S6 in the supplemental information online). The prevalence of extraordinary PMRs is consistent with frequent reports of synchrony in malaria infections (reviewed in [31,34]) and suggests that inflated PMRs will often be an issue.

Estimated PMRs depend critically on the timing of sampling

The sensitivity of estimated PMRs to sampling schedules extends beyond the typically unknown initial parasite age distribution to encompass variation in sampling time. Whether iRBC abundance is quantified from humans or animal models, it is not feasible to sample an entire treatment group simultaneously. Even small shifts in sampling time mean large changes in circulating iRBC abundance, increasing variation in PMRs estimated early versus late in a sampling window (Figure 3). As before, a combination of sequestration and synchrony generate large changes in circulating iRBC abundance, especially when the initial median parasite age is around 12 h. Wide sampling windows are likely to generate substantial variation in PMRs estimated from identical replicate infections (e.g., ±3 h, Figure S7A in the supplemental information online). Narrow sampling windows minimize the variation in estimated PMRs but may be difficult to achieve in practice (±12 min, Figure S7B in the supplemental information online). As a result, a treatment

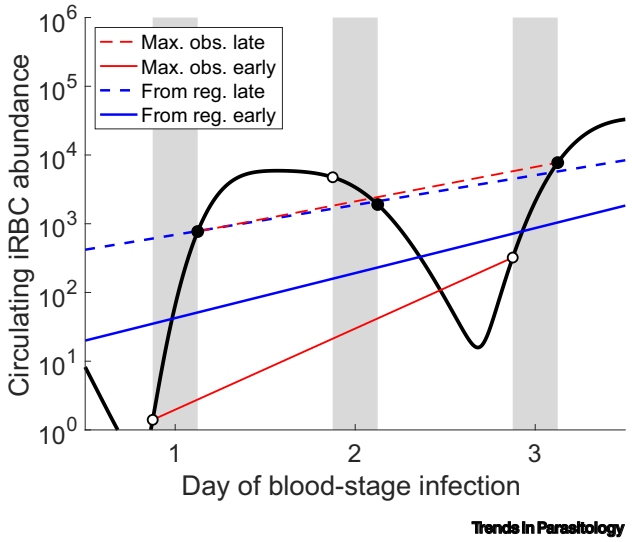

Figure 3. The width of the sampling window substantially alters estimates of the parasite multiplication rate (PMR). When sampling occurs earlier or later than the target time (here, at 1, 2, and 3 days), it encompasses rapid changes in counts of circulating infected red blood cells (iRBCs) (unbroken black circles occur late and open black circles occur early), leading to variability in max. PMR_{obs} (red) and PMR_{reg} (blue). The unbroken lines are from early measurements, and the broken lines are from late measurements. See Box S1 in the supplemental information online for code and data used to generate this figure.

group may exhibit artificially inflated variability in estimated PMRs, even if circulating iRBC abundance is identical across replicate infections and can be measured with no sampling error.

The variability of estimated PMRs simply due to small shifts in sampling time may obscure real differences in PMRs, whether those differences result from environmental or genetic variation. Although estimated PMRs across narrow sampling windows (±6 min) can distinguish quite different true PMRs (6 vs. 12), larger sampling windows (e.g., 6 h) cannot (Figure 4A and B vs. C and D, respectively). More similar true PMRs require finer sampling windows to distinguish (Figure S8A,B in the supplemental information online), especially for maximum observed PMRs (Figure S8A in the supplemental information online) due to the extreme variation in PMR_{obs} through time (Figure 3, Figure S7 in the supplemental information online). While regression methods to estimate PMR routinely outperform those calculated directly from iRBC abundance, strains with similar PMRs remain difficult to distinguish, especially when the initial median parasite age is below 24 h (Figure S8B in the supplemental information online). Thus, the uncertainty in estimated PMRs may both vastly misrepresent the true multiplication rate of a strain and make distinct multiplication rates appear similar.

Spurious PMRs may be widespread

PMRs are widely used, including to evaluate inoculation methods, vaccine efficacy, and antimalarial drug activity in CHI trials [9,16,32], but it has proven difficult to link PMRs with clinical outcomes (reviewed in [18]). Part of that difficulty is likely related to the challenge highlighted here, that existing methods return spuriously large estimates of PMRs *in vivo*. The problem is not sequestration *per se*, but rather that – because of sequestration – small changes in the parasite

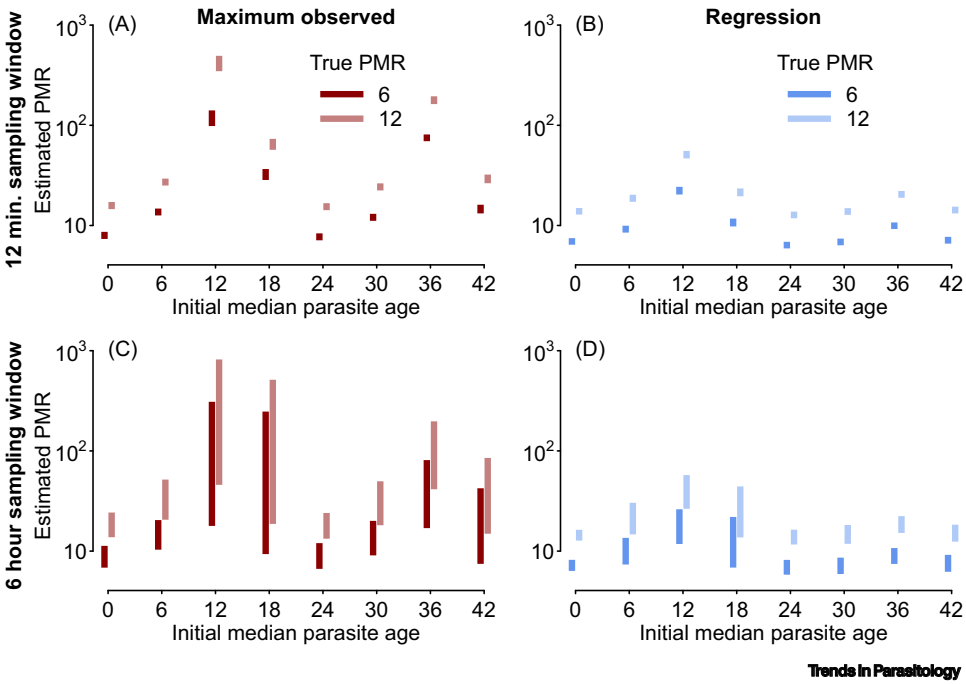

Figure 4. Larger sampling windows render differences in the parasite multiplication rate (PMR) indistinguishable. PMRs were estimated from simulated counts of infected red blood cells (iRBCs) via PMR_{obs} (red, A,C) and PMR_{reg} (blue, B,D) while varying the duration of the sampling window. In the top panels, an infection with a true PMR = 6 is compared with one whose true PMR = 12 for a 12-min window (target time ±6 min), either using PMR_{obs} (A) or PMR_{reg} (B). In both cases, all PMRs can be distinguished. Those differences cannot always be distinguished with a 6 h sampling window (i.e., target time ±3 h, C,D). For example, differences can be detected when the initial median parasite age is 24 h, but not when it is 18 h. Note the log-scale of the y-axes. See Box S1 in the supplemental information online for code and data used to generate this figure.

age distribution can lead to enormous apparent changes in circulating iRBC counts (Figure 2). Synchrony influences the parasite age distribution, leading to sharp oscillations in the fraction of iRBCs that circulate (Figure 1A). Due to sequestration, PMRs estimated from even modestly synchronized infections are likely overestimates, with the magnitude of the error depending on the timing of sampling with respect to the initial parasite age distribution and the level of synchrony. Even when PMRs appear reasonable, apparent differences in PMRs – for example, across strains or hosts – may instead result from variation in synchrony or in the timing of sampling (Figure 4), and thus preclude understanding of this fundamental parasite trait.

Sequestration is impossible in artificial culture, so PMRs should remain reasonable. Accordingly, PMRs typically fall below 15 *in vitro* [10,35,36], values that seem plausible given that median burst sizes range from 15 to 18 [6]. In contrast, Wockner *et al.* [14] estimate *in vivo* PMRs ranging from 28.7 to 35.4 for 3D7, a *P. falciparum* strain with a reported PMR of approximately 8 *in vitro* [11]. While *in vitro* estimates may deviate from true burst sizes *in vivo*, the differences would have to be considerable to explain the data (Figure 1). Thus, extraordinary PMRs are difficult to explain except as spurious artifacts that emerge from sequestration whenever infections are even modestly synchronized (Figure 2). That we and others so often observe extraordinary PMRs *in vivo* makes sense given that infections are often reported to be synchronized within human hosts (reviewed in [31,34]). Spurious PMRs may be widespread, and as PMRs are important for quantification of transmission potential and immune control, this dramatically limits understanding of within-host dynamics.

While it is widely understood that PMRs are not representative of the entire population of parasites due to sequestration [18], we emphasize a more fundamental issue, that the error in iRBC estimates – and hence in PMR – is exquisitely sensitive to small changes in the timing of parasite development or sampling. Thus, the developmental timing and synchrony strongly influence the circulating portion of the iRBC population, and information on synchrony could therefore dramatically improve estimates of total iRBC abundance and PMRs. Unfortunately, estimating synchrony is itself difficult, both due to sequestration and because synchrony estimates tend to be biased by multiplication rates [31]. Considering synchrony and multiplication rates as independent processes generates the bias of current regression methods (Figures 1 and 2). The most promising path forward is to estimate PMRs by fitting semi-mechanistic models to data (e.g., [37]). To avoid spuriously large PMRs, a model would need to incorporate sequestration and dynamic feedbacks between changing synchrony and multiplication rates, ideally using an approach that estimates parameter distributions across individuals (e.g., hierarchical Bayesian methods, [38]). Individual infections could vary in the initial median parasite age and level of synchrony, the speed at which synchrony decays, and the duration of intraerythrocytic development; if unaccounted for, that individual variation could bias PMR estimates.

Concluding remarks

Since the fraction of iRBCs circulating *in vivo* varies wildly through time, it is difficult to be confident in any particular estimate of iRBC abundance. Much of what is understood to be true about malaria parasites rests on estimates of *in vivo* iRBC abundance and multiplication rates. That list includes how the risk of severe health outcomes scales with parasite biomass [1,39], how immune defenses respond to parasite dynamics [33,38,40–41], the potential for adaptive evolution [42,43], and the ability to detect markers of drug resistance in infections [19]. In addition, malaria parasites, along with all Apicomplexans and a number of other pathogenic organisms, face a trade-off between investing resources into replication within the host versus the production of specialized transmission forms (known as transmission investment, reviewed in [44,45]). Since the resolution of that trade-off influences disease severity and spread, a large body of research

Outstanding questions

Methodological barriers

How can models accurately evaluate intraerythrocytic development time, PMR, and synchrony from data?

How much biological detail needs to be included to enable models to accurately estimate PMRs from data?

Data from how many intraerythrocytic cycles is needed to accurately quantify PMRs?

Do existing methods for quantifying PMR accurately estimate the duration of the proliferative cycle (i.e., intraerythrocytic development)?

Do reports of short, noncircadian cycle lengths represent real variation or are they an artifact of methods?

When is a constant PMR sufficient to describe infection dynamics?

Variation driving apparent differences in PMRs

How much do strains vary in their PMRs versus other traits like synchrony?

How much does the timing and degree of sequestration vary across malaria strains?

Does synchrony – and hence the apparent PMR – vary with inoculation route (blood-stage inoculation vs. mosquito bite)?

How often do infections begin synchronously, and, if so, over what time period does synchrony persist?

How much variation is there in the above traits – PMR, synchrony, sequestration – across malaria species (e.g., *P. falciparum* vs. *Plasmodium chabaudi*)?

Effect of PMR on outcomes

How does PMR impact the likelihood that mutations of concern (e.g., drug resistance) will arise *de novo* within an infection?

How do PMRs influence persistence within the host?

has focused on transmission investment in malaria parasites [12,44,46–52]. However, methods for quantifying transmission investment rely on accurate estimates of iRBC abundance [53,54]. That robust estimates of parasite abundance are not currently obtainable, even in the well-studied system of malaria, raises the possibility that important aspects of the biology of pathogenic organisms remain misunderstood (see Outstanding questions).

These issues will arise in any system in which some parts of the life cycle are easier to sample than others and age distributions vary through time. For example, PMRs from *Plasmodium vivax* infections could likewise represent overestimates, since mature iRBCs can still sequester, though at a lower rate than *P. falciparum* (reviewed in [55]). These methodological problems are avoided when fold-increases are measured *in vitro*, for example, PMRs from clinical isolates [10], or replicative capacity in HIV (reviewed in [2]). While *in vitro* methods can reveal genetic diversity in parasites and pathogens, methods for quantifying multiplication rates *in vivo* are urgently needed, since that is a prerequisite for understanding host immune responses and pathology.

Do larger PMRs result in greater disease severity, as predicted by theory?

How do inaccuracies in PMRs alter the estimates of the role of immune defenses, especially those acting early in infection?

How do spuriously large PMRs alter estimates of investment into transmission-stage production, especially early in infection?

How do PMRs relate to the timing of symptom onset?

How does the timing of development and sequestration alter the likelihood that an infection will be detected with rapid diagnostic tests?

Acknowledgments

We thank Tsukushi Kamiya, Anthony Krueger, Nicole Mideo, Damie Pak, Sarah Reece, and Petra Schneider for helpful discussion. We thank Drs Geoffrey M. Jeffery and William E. Collins for provision of the malariatherapy data. This work was supported by the Cornell University College of Agricultural Sciences (M.A.G.) and by NSF Grants 1853495 and 2029262 (L.M.C.).

Declaration of interests

The authors declare no competing interests.

Supplemental information

Supplemental information associated with this article can be found online at https://doi.org/10.1016/j.pt.2023.05.006.

References

1. Mackinnon, M.J. and Read, A.F. (2004) Virulence in malaria: an evolutionary viewpoint. *Philos. Trans. R. Soc. Lond. Ser. B Biol. Sci.* 359, 965–986
2. Fraser, C. *et al.* (2014) Virulence and pathogenesis of HIV-1 infection: an evolutionary perspective. *Science* 343, 1243727
3. Day, T. and Read, A.F. (2016) When does high-dose antimicrobial chemotherapy prevent the evolution of resistance? *PLoS Comput. Biol.* 12, e1004689
4. White, N.J. *et al.* (1992) The effects of multiplication and synchronicity on the vascular distribution of parasites in falciparum malaria. *Trans. R. Soc. Trop. Med. Hyg.* 86, 590–597
5. Simpson, J.A. *et al.* (2002) Population dynamics of untreated *Plasmodium falciparum* malaria within the adult human host during the expansion phase of the infection. *Parasitology* 124, 247–263
6. Reilly, H.B. *et al.* (2007) Quantitative dissection of clone-specific growth rates in cultured malaria parasites. *Int. J. Parasitol.* 37, 1599–1607
7. Allen, R.J.W. and Kirk, K. (2010) *Plasmodium falciparum* culture: the benefits of shaking. *Mol. Biochem. Parasitol.* 169, 63–65
8. Reece, S.E. *et al.* (2010) Stress, drugs and the evolution of reproductive restraint in malaria parasites. *Proc. R. Soc. B Biol. Sci.* 277, 3123–3129
9. Duncan, C.J.A. and Draper, S.J. (2012) Controlled human blood stage malaria infection: current status and potential applications. *Am. J. Trop. Med. Hyg.* 86, 561–565
10. Ribacke, U. *et al.* (2013) Improved *in vitro* culture of *Plasmodium falciparum* permits establishment of clinical isolates with preserved multiplication, invasion and rosetting phenotypes. *PLoS ONE* 8, e69781
11. Murray, L. *et al.* (2017) Multiplication rate variation in the human malaria parasite *Plasmodium falciparum*. *Sci. Rep.* 7, 6436
12. Rono, M.K. *et al.* (2018) Adaptation of *Plasmodium falciparum* to its transmission environment. *Nat. Ecol. Evol.* 2, 377–387
13. Andrade, C.M. *et al.* (2020) Increased circulation time of *Plasmodium falciparum* underlies persistent asymptomatic infection in the dry season. *Nat. Med.* 26, 1929–1940
14. Wockner, L.F. *et al.* (2020) Growth rate of *Plasmodium falciparum*: analysis of parasite growth data from malaria volunteer infection studies. *J. Infect. Dis.* 221, 963–972
15. Barry, A. *et al.* (2021) Higher gametocyte production and mosquito infectivity in chronic compared to incident *Plasmodium falciparum* infections. *Nat. Commun.* 12, 2443
16. Minassian, A.M. *et al.* (2021) Reduced blood-stage malaria growth and immune correlates in humans following RH5 vaccination. *Med* 2, 701–719.e19
17. Woolley, S.D. *et al.* (2021) Development and evaluation of a new *Plasmodium falciparum* 3D7 blood stage malaria cell bank for use in malaria volunteer infection studies. *Malar. J.* 20, 93
18. Gnangnon, B. *et al.* (2021) Deconstructing the parasite multiplication rate of *Plasmodium falciparum*. *Trends Parasitol.* 37, 922–932
19. Mideo, N. *et al.* (2013) Ahead of the curve: next generation estimators of drug resistance in malaria infections. *Trends Parasitol.* 29, 321–328
20. Delley, V. *et al.* (2000) What does a single determination of malaria parasite density mean? A longitudinal survey in Mali. *Tropical Med. Int. Health* 5, 404–412
21. Dobaño, C. *et al.* (2007) Expression of merozoite surface protein markers by *Plasmodium falciparum*-infected erythrocytes in peripheral blood and tissues of children with fatal malaria. *Infect. Immun.* 75, 643–652
22. Färnert, A. *et al.* (1997) Daily dynamics of *Plasmodium falciparum* subpopulations in asymptomatic children in a holoendemic area. *Am. J. Trop. Med. Hyg.* 56, 538–547
23. Dondorp, A.M. *et al.* (2005) Estimation of the total parasite biomass in acute falciparum malaria from plasma PfHRP2. *PLoS Med.* 2, 0788–0797

24. Garnham, P.C.C. (1966) *Malaria Parasites and Other Haemosporidia*, Blackwell Scientific Publications
25. Peters, M.A.E. *et al.* (2021) Challenges in forming inferences from limited data: a case study of malaria parasite maturation. *J. R. Soc. Interface* 18, 20210065
26. Gravenor, M.B. *et al.* (2002) A model for estimating total parasite load in falciparum malaria patients. *J. Theor. Biol.* 217, 137–148
27. Archer, N.M. *et al.* (2018) Resistance to *Plasmodium falciparum* in sickle cell trait erythrocytes is driven by oxygen-dependent growth inhibition. *Proc. Natl. Acad. Sci. U. S. A.* 115, 7350–7355
28. Kriek, N. *et al.* (2003) Characterization of the pathway for transport of the cytoadherence-mediating protein, pfemp1, to the host cell surface in malaria parasite-infected erythrocytes. *Mol. Microbiol.* 50, 1215–1227
29. Weijer, C. (1999) Another tuskegee? *Am. J. Trop. Med. Hyg.* 61, 1–3
30. Schneider, P. *et al.* (2005) Real-time nucleic acid sequence-based amplification is more convenient than real-time PCR for quantification of *Plasmodium falciparum*. *J. Clin. Microbiol.* 43, 402–405
31. Greischar, M.A. *et al.* (2019) The challenge of quantifying synchrony in malaria parasites. *Trends Parasitol.* 35, 341–355
32. Gaur, A.H. *et al.* (2020) Safety, tolerability, pharmacokinetics, and antimalarial efficacy of a novel *Plasmodium falciparum* ATP4 inhibitor SJ733: a first-in-human and induced blood-stage malaria phase 1a/b trial. *Lancet Infect. Dis.* 20, 964–975
33. Metcalf, C.J.E. *et al.* (2011) Partitioning regulatory mechanisms of within-host malaria dynamics using the effective propagation number. *Science* 333, 984–988
34. Mideo, N. *et al.* (2013) The Cinderella Syndrome: Why do malaria-infected cells burst at midnight? *Trends Parasitol.* 29, 10–16
35. Amoah, L.E. *et al.* (2020) Comparative analysis of asexual and sexual stage *Plasmodium falciparum* development in different red blood cell types. *Malar. J.* 19, 200
36. Stewart, L.B. *et al.* (2020) Intrinsic multiplication rate variation and plasticity of human blood stage malaria parasites. *Commun. Biol.* 3, 624
37. Wattanakul, T. *et al.* (2021) Semimechanistic pharmacokinetic and pharmacodynamic modeling of piperaquine in a volunteer infection study with *Plasmodium falciparum* blood-stage malaria. *Antimicrob. Agents Chemother.* 65, e01583-20
38. Kamiya, T. *et al.* (2021) Linking functional and molecular mechanisms of host resilience to malaria infection. *eLife* 10, e65846
39. Cunnington, A.J. *et al.* (2013) Stuck in a rut? Reconsidering the role of parasite sequestration in severe malaria syndromes. *Trends Parasitol.* 29, 585–592
40. Metcalf, C.J.E. *et al.* (2012) Revealing mechanisms underlying variation in malaria virulence: effective propagation and host control of uninfected red blood cell supply. *J. R. Soc. Interface* 9, 2804–2813
41. Kamiya, T. *et al.* (2020) Uncovering drivers of dose-dependence and individual variation in malaria infection outcomes. *PLoS Comput. Biol.* 16, e1008211
42. Chang, H.H. *et al.* (2013) Malaria life cycle intensifies both natural selection and random genetic drift. *Proc. Natl. Acad. Sci. U. S. A.* 110, 20129–20134
43. Chang, H.H. and Hartl, D.L. (2014) Recurrent bottlenecks in the malaria life cycle obscure signals of positive selection. *Parasitology* 142, S98–S107
44. Koella, J.C. and Antia, R. (1995) Optimal pattern of replication and transmission for parasites with two stages in their life cycle. *Theor. Popul. Biol.* 47, 277–291
45. Smith, T.G. *et al.* (2002) Sexual differentiation and sex determination in the Apicomplexa. *Trends Parasitol.* 18, 315–323
46. Bruce, M.C. *et al.* (1990) Commitment of the malaria parasite *Plasmodium falciparum* to sexual and asexual development. *Parasitology* 100, 191–200
47. McKenzie, F.E. and Bossert, W.H. (1998) The optimal production of gametocytes by *Plasmodium falciparum*. *J. Theor. Biol.* 193, 419–428
48. Mideo, N. and Day, T. (2008) On the evolution of reproductive restraint in malaria. *Proc. R. Soc. B Biol. Sci.* 275, 1217–1224
49. Pollitt, L.C. *et al.* (2011) Competition and the evolution of reproductive restraint in malaria parasites. *Am. Nat.* 177, 358–367
50. Greischar, M.A. *et al.* (2016) Predicting optimal transmission investment in malaria parasites. *Evolution* 70, 1542–1558
51. Greischar, M.A. *et al.* (2019) Partitioning the influence of ecology across scales on parasite evolution. *Evolution* 73, 2175–2188
52. Stewart, L.B. *et al.* (2022) *Plasmodium falciparum* sexual commitment rate variation among clinical isolates and diverse laboratory-adapted lines. *Microbiol. Spectrum* 10, e0223422
53. Eichner, M. *et al.* (2001) Genesis, sequestration and survival of *Plasmodium falciparum* gametocytes: parameter estimates from fitting a model to malariatherapy data. *Trans. R. Soc. Trop. Med. Hyg.* 95, 497–501
54. Greischar, M.A. *et al.* (2016) Quantifying transmission investment in malaria parasites. *PLoS Comput. Biol.* 12, e1004718
55. Silva-Filho, J.L. *et al.* (2020) *Plasmodium vivax* in hematopoietic niches: hidden and dangerous. *Trends Parasitol.* 36, 447–458
56. Khoury, D.S. *et al.* (2014) Effect of mature blood-stage *Plasmodium* parasite sequestration on pathogen biomass in mathematical and in vivo models of malaria. *Infect. Immun.* 82, 212–220
57. Kilian, A.H. *et al.* (2000) Reliability of malaria microscopy in epidemiological studies: results of quality control. *Trop. Med. Int. Health* 5, 3–8